frontiers | Frontiers in Space Technologies

TYPE Original Research
PUBLISHED 03 July 2023
DOI 10.3389/frspt.2023.1162268

OPEN ACCESS

EDITED BY
Corey Nislow,
University of British Columbia, Canada

REVIEWED BY
Jeffrey C. Petruska,
University of Louisville, United States
Carlos De Almeida,
University of Louisville, in collaboration with reviewer JP
Martin Katz,
University of Missouri, United States

*CORRESPONDENCE
Masaaki Yoshikawa,
yoshikawa-ma@cc.osaka-dent.ac.jp

RECEIVED 21 February 2023
ACCEPTED 05 June 2023
PUBLISHED 03 July 2023

CITATION
Yoshikawa M, Matsukawa M, Oshima H, Ishikawa C, Li H, Kudo T, Shiba D, Shirakawa M, Muratani M, Takahashi S, Uemura M, Aizawa S and Shiga T (2023), Comparing the effects of microgravity and amyotrophic lateral sclerosis on mouse dorsal root ganglia.
Front. Space Technol. 4:1162268.
doi: 10.3389/frspt.2023.1162268

Comparing the effects of microgravity and amyotrophic lateral sclerosis on mouse dorsal root ganglia

Masaaki Yoshikawa[1,2]*, Mutsumi Matsukawa[1], Hideki Oshima[3], Chihiro Ishikawa[4], Haiyan Li[4], Takashi Kudo[5], Dai Shiba[6], Masaki Shirakawa[6], Masafumi Muratani[7], Satoru Takahashi[5], Mamoru Uemura[2], Shin Aizawa[1] and Takashi Shiga[4,8]

[1]Division of Anatomical Science, Department of Functional Morphology, Nihon University School of Medicine, Tokyo, Japan, [2]Department of Anatomy, Osaka Dental University, Osaka, Japan, [3]Division of Neurosurgery, Department of Neurological Surgery, Nihon University School of Medicine, Tokyo, Japan, [4]Laboratory of Neurobiology, Graduate School of Comprehensive Human Sciences, University of Tsukuba, Ibaraki, Japan, [5]Department of Anatomy and Embryology, Institute of Medicine, University of Tsukuba, Ibaraki, Japan, [6]JEM Utilization Center, Human Spaceflight Technology Directorate, Japan Aerospace Exploration Agency (JAXA), Ibaraki, Japan, [7]Department of Genome Biology, Institute of Medicine, University of Tsukuba, Ibaraki, Japan, [8]Department of Neurobiology, Faculty of Medicine, University of Tsukuba, Ibaraki, Japan

Introduction: Microgravity (MG) exposure causes motor deficits and decreased neuronal activity, effects that resemble the ones observed in motor neuron diseases such as amyotrophic lateral sclerosis (ALS). Several recent studies have shown that exposure to MG and ALS also impacts the sensory systems. Yet, the role of sensory impairment in this degenerative process of exposure to MG and ALS remains unknown. In this study, we aimed at elucidating how the sensory system is affected by exposure to MG and ALS.

Methods: To this end, we compared gene expression in the mouse lumbar dorsal root ganglia (DRG) of MG-exposed animals with that of control animals that remained under artificial gravity conditions. We then investigated the effects of the human superoxide dismutase 1 (SOD1) G93A mutation in a mouse model of ALS ($SOD1^{G93A}$ mice) on gene expression in the DRG.

Results: The overlap of genes with negatively correlated expression was greater than those with positively correlated expression between the DRG of MG-exposed and $SOD1^{G93A}$ mice. Additionally, genes related to Imoonglia (characteristics of both immune and glial cells) and macrophage increased in response to MG exposure, while satellite glial cell genes were expressed in response to SOD1 mutation. Next, we examined genes related to sensory neuron subtypes in the DRG. We found altered gene expression in genes related to proprioceptive and mechanoreceptive neurons in the DRG of MG-exposed and $SOD1^{G93A}$ mice. Remarkably, the expression of *Atf3* and genes related to nociceptive neurons in the DRG of $SOD1^{G93A}$ mice at postnatal day (P) 120 was considerably altered, whereas MG-exposed and $SOD1^{G93A}$ mice at P30 presented little changes.

Discussion: These results indicate that exposure to MG and ALS affect gene expression in genes related to neurons and non-neuronal cells in the DRG, with significant differences between the effects of MG and the SOD1 mutation. Elucidation of the impact of exposure to MG and ALS pathogenesis in the

DRG, including identification of the molecular pathways that regulate DRG dysfunction, will help better understand the differences in vulnerability and the triggering processes of impaired motor function associated with MG and ALS.

KEYWORDS

microgravity, amyotrophic lateral sclerosis, dorsal root ganglion neuron, proprioceptor, cutaneous low-threshold mechanoreceptor, nociceptor, satellite glial cell, lmoonglia

1 Introduction

Microgravity (MG) exposure and amyotrophic lateral sclerosis (ALS) are characterized by common alterations in the skeletal muscle, motor, nervous, vasculature, and immune systems, leading to motor deficits, including muscle atrophy and loss of neuronal activity (Vinsant et al., 2013a; Vinsant et al., 2013b; Clément and Wood, 2014; Rizzo et al., 2014; Gunes et al., 2020; Yu et al., 2020; Buoite Stella et al., 2021; Okada et al., 2021; Yoshikawa et al., 2022a; Yoshikawa et al., 2022b). Exercise on the ground can reverse motor neuron and muscle abnormalities caused by exposure to MG, whereas the degeneration in ALS is irreversible and motor neuron death cannot be recovered. Sensory neurons consist of various subtypes of neurons that respond to external stimuli and the internal state of bodies; these neurons are mediators of nociception, mechanoreception, and proprioception (Meltzer et al., 2021). Changes in gravity alter the sensory input from the vestibular system, which consequently generates mismatches between the expected and actual sensory vestibular inputs during active movements (Carriot et al., 2021). Furthermore, studies have shown that exposure to MG induces changes in structures and neuronal gene expressions in the brain and spinal cord (Carriot et al., 2021; Yoshikawa et al., 2022b; Holley et al., 2022; Mammarella et al., 2022). However, the alterations occurring in the sensorimotor system due to gravitational changes and the adaptation of sensory neurons during spaceflight have not been fully unraveled nor have the molecular mechanisms underlying these effects.

ALS is a neurodegenerative disease that causes muscle atrophy and weakness associated with gradual motor neuron degeneration, for which no clear explanation for ALS pathogenesis is available thus far (Vinsant et al., 2013a). There is still no treatment to cure ALS, and current treatments can only slow its progression and improve the patient's comfort. In humans, some forms of ALS are caused by mutations in the superoxide dismutase 1 (*SOD1*) gene, the transactive response DNA-binding protein 43-kDa (*TDP-43*) gene, the fused in sarcoma (*FUS*) gene, and several other genes (Chia et al., 2018; Kim et al., 2020). In animal models carrying a mutant SOD1 gene, ALS develops because of the toxicity of the mutant protein (Chia et al., 2018; Kim et al., 2020). Sensory systems are considered less vulnerable than motor systems, and potential sensory involvement is overlooked as a feature of ALS. However, there have been reported cases of ALS patients with sensory deficits and many patients experience pain (Iglesias et al., 2015). Abnormalities in sensory nerve fibers and satellite glial cells (SGCs) of sensory neurons in ALS animal models have also been reported (Guo et al., 2009; Sábado et al., 2014; Ruiz-Soto et al., 2020). Additionally, altered gene expression of solute carrier (SLC) transporters, resulting in neurodegeneration, was observed in MG and ALS mouse models (Hu et al., 2020; Paul et al., 2021; Latif and Kang, 2022; Yoshikawa et al., 2022a; b). While exposure to MG and ALS are characterized by commonly observed alterations in the motor system, only a few reports have described the molecular changes underlying sensory neuron dysfunction in ALS or after exposure to MG (Nagatomo et al., 2014; Sábado et al., 2014; Iglesias et al., 2015; Rubio et al., 2022). Moreover, changes in the gene expression in peripheral nervous systems in this degenerative process of exposure to MG and ALS remains unknown. Therefore, to elucidate the sensory systems affected by exposure to MG or ALS, we investigated the effects of exposure to MG and mutant SOD1 on gene expression in the mouse dorsal root ganglia (DRG). Altered gene expression in MG-exposed and ALS models shows similarities and differences that could help to better understand the triggering processes of the disease. Additionally, most MG-exposure-resulting deficits seem to be reversible, which may provide further input to understanding the mechanisms underlying ALS and developing new therapeutics.

2 Materials and methods

2.1 Microgravity animals

All experiments were approved by the Institutional Animal Care and Use Committee of the University of Tsukuba, JAXA, Explore Biolabs, and NASA and were conducted according to the applicable guidelines in Japan and the United States of America. The mice and the treatments have been described in previous studies (Shiba et al., 2017; Matsumura et al., 2019). Briefly, 12 male mice (8-week-old, C57BL/6J) were singly housed for 35 days under MG (n = 6) or artificial gravity (AG, n = 6) at 1 × g centrifugation in the International Space Station. By comparing the effects of MG with those of AG, we differentiated the effects of MG from other effects such as radiation. Two days after splashing down, the 13-week-old mice were euthanized and dissected in the laboratory for tissue collection. For RNA-sequencing analysis (RNA-seq), three male MG-exposed mice with decreased soleus/gastrocnemius muscle weight and three male AG-exposed controls with maintained muscle weight were compared to six male ground control mice that were not exposed to either MG or AG (Shiba et al., 2017; Okada et al., 2021).

2.2 Amyotrophic lateral sclerosis animals

All experiments conformed to the ARRIVE and National Institutes of Health guidelines and were approved by the Institutional Animal Care and Use Committee of the Nihon

University School of Medicine. Wild type (WT) females and SOD1^{G93A} males [B6SJL-TgN(SOD1*^{G93A})1Gur], obtained from The Jackson Laboratory (Bar Harbor, ME, USA), were bred to generate SOD1^{G93A} mice (Ludolph et al., 2010). Genotyping was performed using standard primers against mutant *SOD1*. The primers for mutant *SOD1* were forward (oIMR0113) 5′-CAT CAGCCCTAATCCATCTGA-3′ and reverse (oIMR0114) 5′-CGC GACTAACAATCAAAGTGA-3′ and those for the internal control were forward (oIMR7338) 5′-CTAGGCCACAGAATTGAAAGA TCT-3′ and reverse (oIMR7339) 5′-GTAGGTGGAAATTCTAGC ATCATCC-3′ (Gurney et al., 1994).

2.3 Dorsal root ganglia dissection

MG- and AG-exposed (13-week-old), SOD1^{G93A}, and WT mice (postnatal day 30 and 120; P30 and P120) mice were decapitated under deep anesthesia using isoflurane (Escain, Pfizer, Tokyo, Japan) and their lumbar spinal columns, including the DRG, were dissected. All lumbar spinal column samples were stored at −80 °C until use. After freezing, the samples were incubated overnight at 4°C in RNAlater (Sigma Aldrich, St. Louis, MO, USA) to prevent RNA degradation during tissue thawing. Individual DRG from lumbar 1 to 5 were extracted from the intervertebral foramina.

2.4 RNA-Sequencing

RNA-sequencing was performed as previously described (Ikeda et al., 2019; Matsumura et al., 2019). Briefly, lumbar DRG samples from MG- and AG-exposed, SOD1^{G93A}, and WT mice (n = 3, respectively) were individually homogenized in RNAiso Plus (Takara Bio, Shiga, Japan) using the BioMasher II (Nippi Inc., Tokyo, Japan) and QIAshredder (Qiagen, Hilden, Germany). Pooled samples from each animal were processed separately for sequencing. Total RNA was isolated using RNAiso Plus (Takara Bio), according to the manufacturer's protocol. RNA-seq libraries were prepared using the NEBNext Ultra Directional RNA Library Prep Kit (New England Biolabs, Ipswich, MA, USA) after rRNA depletion using the NEBNext rRNA Depletion Kit (New England Biolabs). Paired-end RNA-seq (2 × 36 bp) was then performed on a NextSeq500 platform (Illumina Inc., San Diego, CA, USA) by Tsukuba i-Laboratory LLP (Ibaraki, Japan). FASTQ files were processed using the CLC Genomics Workbench (CLC-GW, version 10.1.1; Qiagen). Sequence reads were imported, and directly used for mapping to the mouse genome (mm10) and the annotated genes were quantified. These processing steps were performed using the default setting provided in CLC-GW as described in user manual. Sequence trimming was not performed, but low-quality score reads were discarded by CLC-GW as file import option, and adaptor reads were minimal as library was size-selected to avoid short or no insert reads. Gene expression values were estimated as total counts normalized by transcripts per million. Genes with 0 counts in any sample were excluded, and differential expression was analyzed using the Empirical Analysis of DGE tool (EDGE test) in the CLC Main Workbench (version 21.0.3; Qiagen). Differentially expressed genes were extracted among conditions with FDR-corrected $p < 0.05$.

2.5 Gene ontology annotation analysis

Differentially expressed genes (DEGs) with an absolute fold change of >2 and a t-test p-value of <0.05 were imported into the BaseSpace Correlation Engine (Illumina). Gene ontology (GO) terms enriched for the genes of interest in the DRG of MG-exposed and SOD1G93A mice were determined using rank-based enrichment statistics and biomedical ontologies using the BaseSpace Correlation Engine. The BaseSpace Correlation Engine employs a ranked nonparametric analysis strategy driven by a Fisher's test algorithm. A p-value threshold for significance of 0.0001 was used (Elcombe et al., 2022).

2.6 Cell-type-related differentially expressed gene analysis

Using the BaseSpace Correlation Engine, we evaluated the overlap among the DEGs of MG-exposed (compared with AG-exposed) and SOD1^{G93A} (compared with WT) mice at P30 and P120 and cell-type-related marker genes from previous studies (Usoskin et al., 2015; Li et al., 2016; Avraham et al., 2020; 2021; Sharma et al., 2020; Huang et al., 2021; Wu et al., 2021).

2.7 Statistical analysis

All quantitative analyses were performed on three replicates of AG-exposed, MG-exposed, WT, and SOD1^{G93A} mice. For sequencing data, DEGs were determined using the EDGE test ($p < 0.05$, fold change with absolute value >2) in the CLC Main Workbench (Ikeda et al., 2019). All statistical analyses were performed in the BaseSpace Correction Engine; similarities between any two datasets were evaluated as overlapping p-values using the Running Fisher algorithm (Murano et al., 2019). The Bonferroni correction was used to adjust the significance level according to the number of dataset pairs (Murano et al., 2019).

3 Results

3.1 Altered expression of genes related to axonal injury, proprioceptive neurons, immune cells, and glia observed in the dorsal root ganglia of microgravity-exposed and SOD1^{G93A} mice

We performed whole transcriptome analysis on DRG samples from MG- (n = 3) and AG-exposed mice (n = 3) and found 316 differentially expressed genes (DEGs; 138 upregulated and 178 downregulated genes, respectively; Supplementary Dataset S1). The expression of genes related to mechanoreceptive neurons (*Trpc5*), nociceptive neurons (*Zfhx2os*, *Penk*, *Gad1*, *Trpc5*), glia (*Csl*, *Saa3*, *Mog*, *Grin2a*, *Gfap*), neurotrophic factors (*Caps2*, *Fgf10*), serotonergic neurons (*Htr2c*), GABA receptors (*Gabrd*, *Gabrr2*), GABAergic neurons (*Gad1*), neuropeptide receptors (*Trhr*), the SLC family (*Slc39a12*, *Slc4a5*), calcium voltage-gated channels (*Cacng3*), axonal injury (*Ecel1*), and immune cells (*Ulbp1*, *Pdyn*, *Trbc2*) increased in the DRG of MG-exposed mice compared with that of AG-exposed mice (Supplementary Table S1). In contrast, the expression of

genes related to proprioceptive neurons (*Egr3*, *Cntn5*), nociceptive neurons (*Csrp3*, *Ntsr1*), glia (*Fcrls*), neurotrophic factors (*Nrtn*, *Areg*), neuropeptide receptors (*Vipr2*, *Ghsr*), Eph family (*Epha1*), SLC family (*Slc12a3*, *Slc15a3*, *Slc25a31*), axonal injury (*Csrp3*), heat shock proteins (*Hspa1b*), epigenetics (*Gnmt*), and immune cells (*Syk*, *Pou2f2*, *Cd37*, *Cd180*, *Cd52*, *Cd79b*, *Aif1*, *Cd72*, *Batf*, *Fcrl5*) decreased in the DRG of MG-exposed mice (Supplementary Table S1). These results suggest that sensory, glial, and immune system-related genes were altered by MG.

We performed the same analysis in ALS and WT mice and observed 367 DEGs (173 upregulated and 194 downregulated) between SOD1^{G93A} (n = 3) and WT (n = 3) animals at P30 (Supplementary Dataset S1). Neuromuscular junctions were denervated in the tibialis anterior (fast-fatigable type) muscle in SOD1^{G93A} mice at P30 (Vinsant et al., 2013b). The expression of genes related to mechanoreceptive neurons (*Trpc7*, *Nrsn2*), nociceptive neurons (*Trpc7*), neurotrophic factors (*Vgf*), neuropeptides (*Vip*), neuropeptide receptors (*Sstr3*, *Sstr2*), SLC family (*Slc16a14*), heat shock proteins (*Hspb7*, *Hspa1l*), potassium voltage-gated channels (*Kcna5*, *Kcnc3*), axonal injury (*Nfe2*), and immune cells (*Foxp3*, *Trem3*, *Cd200r3*, *Cd209f*, *Cd51*) increased in the DRG of SOD1^{G93A} mice compared with that of WT mice at P30 (Supplementary Table S2). In contrast, the expression of genes related to nociceptive neurons (*Esr2*, *Gad1*, *Mrgpra4*, *Mrgpra6*), glia (*Gfap*, *Mog*, *Olig2*), GABA receptors (*Gabra4*), GABAergic neurons (*Gad1*), SLC family (*Slc10a2*, *Slc1a2*, *Slc6a5*, *Slc16a8*, *Slc5a9*, *Slc18a3*, *Slc6a16*) and immune cells (*Cd4*, *Rag1*, *Cd3e*, *Cd3g*, *Cd8b1*, *Cd7*, *Cd8a*, *Cd6*, *Trbc2*) decreased in the DRG of P30 SOD1^{G93A} mice (Supplementary Table S2). These results suggest that sensory, glial, and immune system-related genes were altered by ALS.

Finally, we analyzed differences in gene expression in ALS and control mice at P120. SOD1^{G93A} mice show progressive paralysis from ~P90 and die at ~ P135 with 50% motor neuron loss (Vinsant et al., 2013a). We found 1514 DEGs between SOD1^{G93A} (n = 3) and WT (n = 3) mice, with 686 genes upregulated and 828 downregulated (Supplementary Dataset S1). The expression of genes related to proprioceptive neurons (*Aldh1a3*), mechanoreceptive neurons (*Itga2*, *Rftn1*, *Cxcr2*, *Trpv4*), nociceptive neurons (*Mrgpra6*, *Osm*, *Alk*, *Osmr*, *Gpx3*, *Trpv4*), glia (*Trem2*, *Saa1*, *Cd163l1*, *Cd68*, *Il7r*, *Runx2*, *Saa3*, *Apod*, *Cebpd*, *Cd200r1*, *Ms4a14*, *Vim*, *Apoe*, *Emp1*, *Gfra1*), neurotrophic factors (*Gdnf*, *Igfbpl1*, *Areg*, *Artn*, *Nell1*, *Fgf3*, *Vgf*, *Bdnf*), neurotrophic receptors (*Met*, *Gfra1*), neuropeptide (*Npy*, *Gal*), neuropeptide receptors (*Npy4r*, *Npy1r*), serotonergic neurons (*Htr2b*), Eph family (*Epha5*), SLC family (*Slc6a4*, *Slc7a11*, *Slc10a6*, *Slc15a3*, *Slc37a2*, *Slc11a1*), potassium voltage-gated channels (*Kcnh4*, *Kcna5*, *Kcnq1 Kcnk6*), voltage-gated sodium channels (*Scn4a*), neurogenesis (*Gadd45a*, *Gadd45g*), axonal injury (*Sprr1a*, *Atf3*, *Ecel1*, *Runx2*, *Sox11*, *Csf2rb2*, *Jun*, *Eif4ebp1*, *Adcyap1*) and immune cells (*Gpnmb*, *Cd28*, *Lgals3*, *Cd68*, *Il7r*, *Itgax*, *Cd4*, *Cd300a*, *Cd300lf*, *Batf*, *Cd48*, *Cd300c2*, *Cd7*, *Cd22*, *Cd36*, *Cd38*) increased in the DRG of SOD1^{G93A} mice compared with WT mice at P120 (Supplementary Table S3). In contrast, the expression of genes related to proprioceptive neurons (*Cntn5*, *Pvalb*), mechanoreceptive neurons (*Mafa*), nociceptive neurons (*Csrp3*), glia (*Prx*, *Mpz*, *Mag*, *Ephb1*, *Mbp*, *Mog*), neurotrophic factors (*Fgfbp1*, *Igfbp2*, *Fgf4*), serotonergic neurons (*Htr3a*, *Htr7*), Eph family (*Epha10*, *Efnb3*, *Ephb1*), GABA receptors (*Gabra2*, *Gabrg1*), SLC family (*Slc25a13*, *Slc2a10*, *Slc6a1*, *Slc25a18*, *Slc6a20a*, *Slc30a10*, *Slc7a11*, *Slc13a3*, *Slc38a5*, *Slc6a9*, *Slc2a12*, *Slc36a2*, *Slc38a3*, *Slc22a6*, *Slc2a5*, *Slc12a5*, *Slc6a11*, *Slc22a8*, *Slc22a2*, *Slc22a22*, *Slc6a5*, *Slc30a3*, *Slc36a1os*, *Slc18a3*, *Slc26a3*, *Slc6a21*), heat shock proteins (*Hspa1l*, *Dnah7c*, *Hspb3*, *Dnajb8*), potassium voltage-gated channels (*Kcnj8*, *Kcnc1*, *Kcnk2*, *Kcns1*, *Kcnj11*, *Kcnc3*, *Kcnk9*, *Kcna7*), voltage-gated sodium channels (*Scn4a*), calcium voltage-gated channels (*Cacna1s*, *Cacng6*), Wnt family (*Wnt4*, *Wnt5b*, *Wnt7b*, *Wnt7a*), axonal injury (*Csrp3*) and immune cells (*Cd74*, *Htr7*, *Cd79a*, *Aif1l*, *Cd19*, *Rag1*) decreased in the DRG of P120 SOD1^{G93A} mice (Supplementary Table S3). These results suggest that genes related to multiple systems, including sensory, glial, and immune systems, were altered by ALS.

3.2 Gene ontology term analysis showed different enrichment patterns in differentially expressed genes of the dorsal root ganglia of between microgravity-exposed and SOD1^{G93A} Mice

To investigate the role of DEGs in the DRG of MG-exposed (compared with AG-exposed) and SOD1^{G93A} (compared with WT) mice, we performed GO analysis using the BaseSpace Correlation Engine (Murano et al., 2017; 2019). First, we compared DEGs of the DRG of MG- and AG-exposed mice and found that "transmembrane transporter complex (upregulated)," "proximal/distal pattern formation (upregulated)," "ion channel activity (upregulated)," "leukocyte activation (downregulated)," "lymphocyte activation (downregulated)," and "receptor complex (downregulated)" were highly enriched in the DEGs of MG-exposed DRG compared to AG-exposed ones (Figure 1).

Next, we compared our ALS model with the WT control and observed the GO terms. "oxygen binding (upregulated)," "transcription factor activity, RNA polymerase II proximal promoter sequence-specific DNA binding (upregulated)," "hemoglobin complex (upregulated)," "adaptive immune response (downregulated)," "immunological synapse (downregulated)," and "T-cell selection (downregulated)" were highly enriched in DEGs of SOD1^{G93A} DRG compared to WT at P30 (Figure 2); and "inflammatory response (upregulated)," "regulation of inflammatory response (upregulated)," "positive regulation of cytokine production (upregulated)," "contractile fiber (downregulated)," "muscle contraction (downregulated)," and "striated muscle cell development (downregulated)" were highly enriched in the DEGs of SOD1^{G93A} DRG compared to WT at P120 (Figure 3).

To investigate whether the DEGs between MG- and AG-exposed mice overlapped with those between SOD1^{G93A} and WT mice at P30, we assessed similarities in gene-expression pattern using the BaseSpace platform. We found that 13 genes were commonly altered in MG-exposed and SOD1^{G93A} mice at P30 (overlap $p = 4.40 \times 10^{-5}$; Figure 4A). The overlap of genes with negatively correlated expression (10 genes) was greater than for those with positively correlated expression (3 genes; Figure 4B), which indicates that the opposite response occurs in the several common genes.

Next, we examined the similarities between DEGs of MG-exposed and SOD1^{G93A} mice at P120. The number of common DEGs increased to 52 genes (overlap $p = 0.10$) at P120 (Figure 4C). The number of overlapping genes with positively correlated expression (27 genes) was comparable those with negatively correlated expression (25 genes; Figure 4D), indicating that the

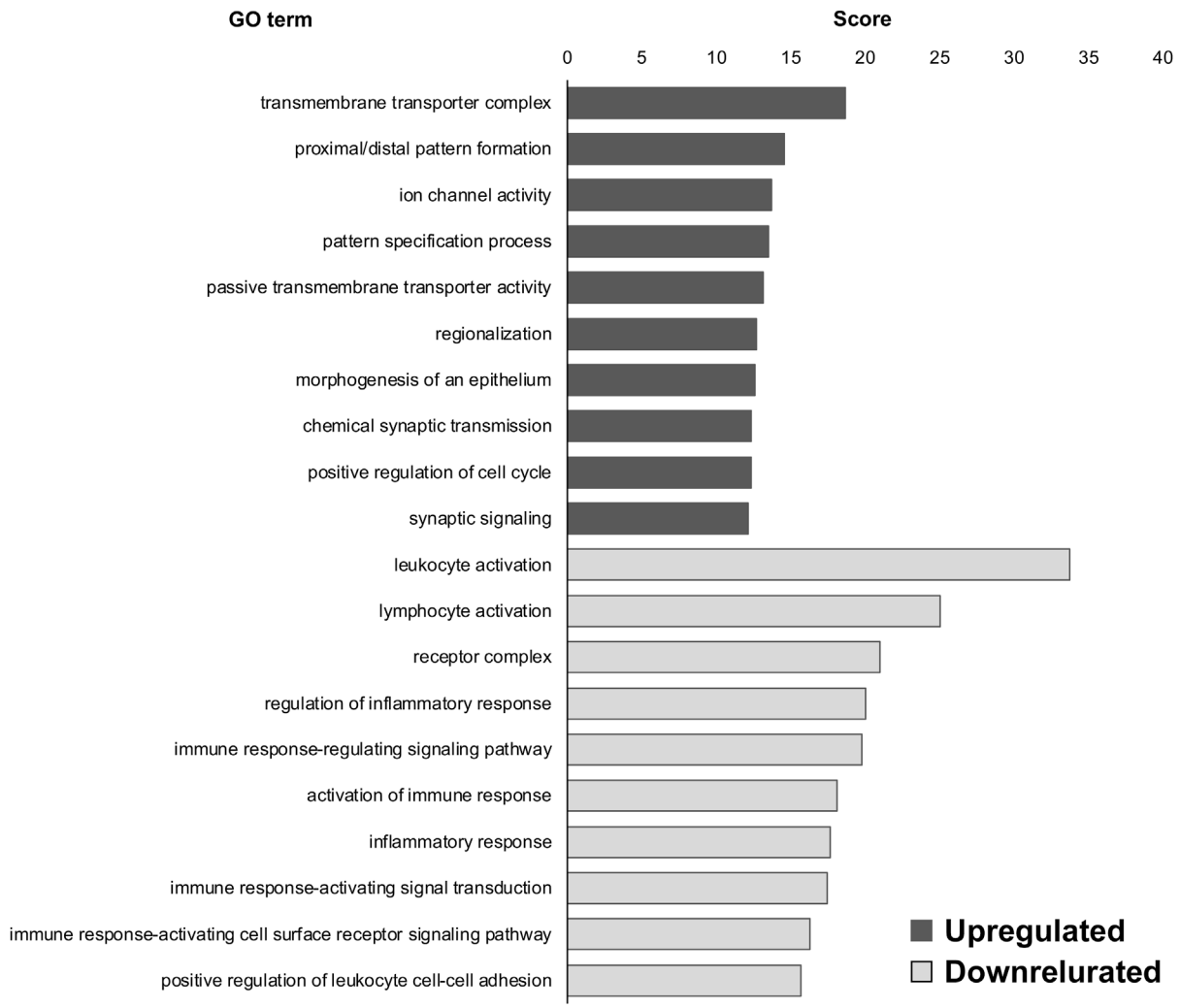

FIGURE 1
Gene ontology (GO) terms of differentially expressed genes (DEGs) in the dorsal root ganglia (DRG) of microgravity (MG)-exposed mice compared to artificial gravity (AG)-exposed mice. Transmembrane transporter complex, proximal/distal pattern formation, and ion channel activity were the upregulated GO terms in the DRG of MG-exposed mice whereas leukocyte activation, lymphocyte activation, and receptor complex were the downregulated GO terms. Scores of the 10 most highly enriched upregulated (gray) and downregulated (white) GO terms revealed changes in the DRG caused by MG exposure.

positive and opposite reactions are mixed in the several common genes. Additionally, we examined the difference between DEGs of $SOD1^{G93A}$ mice at P30 and P120. 62 genes (overlap $p = 0.35$) were common between P30 and P120 (Figure 4E). The number of overlapping positively correlated genes (32 genes) was comparable to negatively correlated genes (30 genes; Figure 4F), indicating that the positive and opposite response in the several common genes is mixed. Finally, we examined the common GO term of MG-exposed and $SOD1^{G93A}$ mice at P30 and P120. Common GO terms indicated that "inflammatory response (MG exposure, downregulated; P30 ALS, downregulated; P120 ALS, upregulated)," "leukocyte activation (MG exposure, downregulated; P30 ALS, upregulated; P120 ALS, upregulated)," "leukocyte migration (MG exposure, downregulated; P30 ALS, downregulated; P120 ALS, upregulated)," "positive regulation of cytokine production (MG exposure, upregulated; P30 ALS, upregulated; P120 ALS, upregulated)" "negative regulation of immune system process (MG exposure, downregulated; P30 ALS, upregulated; P120 ALS, upregulated)," and "adaptive immune response (MG exposure, downregulated; P30 ALS, downregulated; P120 ALS, upregulated)" were highly enriched in DEGs by exposure to MG and ALS ($p < 0.0001$; Figure 5 and Supplementary Dataset S2). While inflammatory response was upregulated in $SOD1^{G93A}$ mice at P120, they were downregulated in MG-exposed and $SOD1^{G93A}$ mice at P30. Upregulated and downregulated GO terms related to immune processes were different among exposure to MG-exposed and $SOD1^{G93A}$ mice at P30 and P120 (Supplementary Dataset S2). These results indicate that exposure to MG and ALS are associated with alterations in inflammation, cytokine production, and immune responses, with the differential responses of gene sets altered in the DRG.

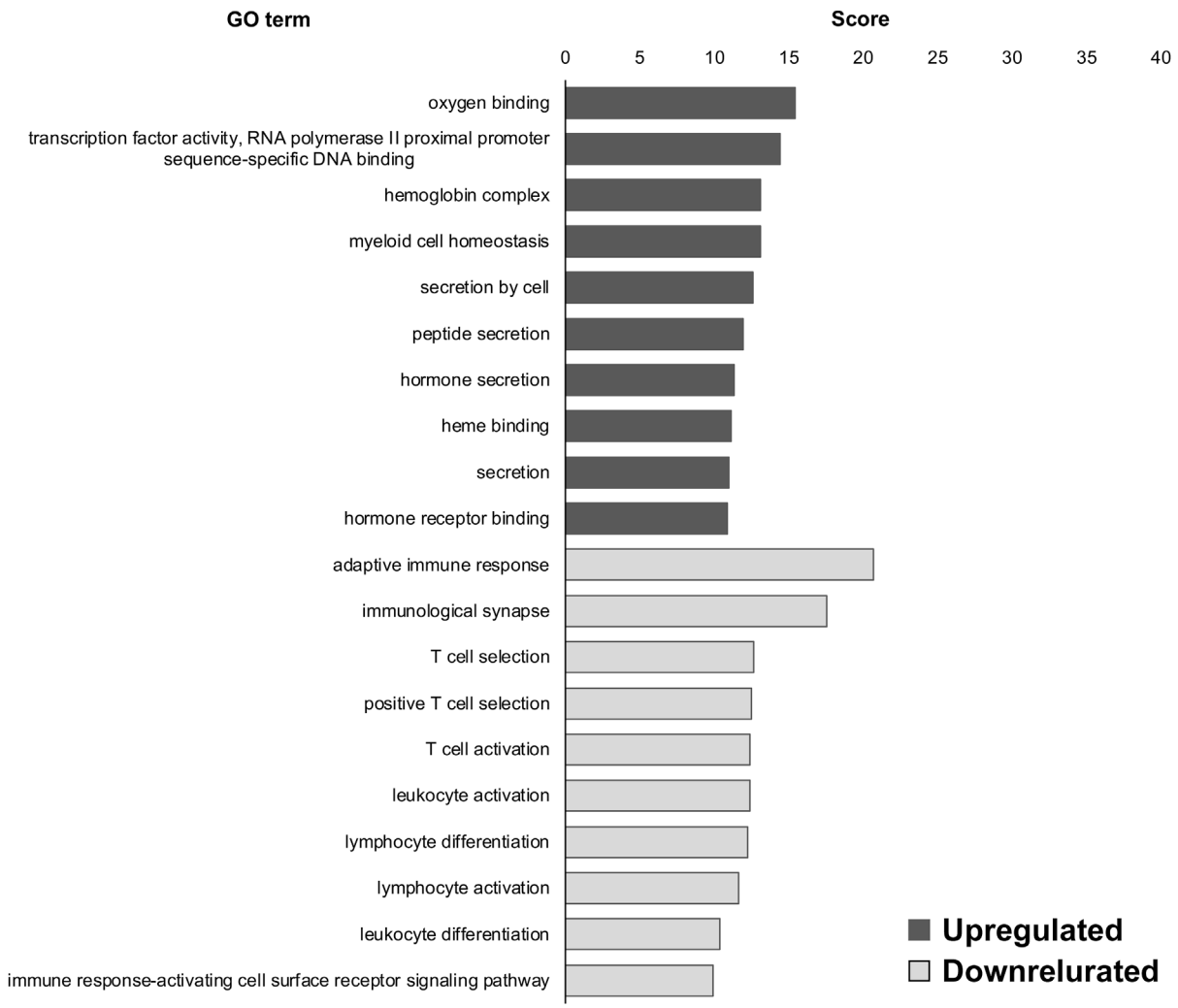

FIGURE 2
GO terms of DEGs in SOD1^{G93A} mice compared to WT mice at P30. Oxygen binding, transcription factor activity, and hemoglobin complex were the upregulated GO terms in the DRG of SOD1^{G93A} mice at P30 whereas adaptive immune response, immunological synapse, and T-cell selection were downregulated GO terms. Scores of the 10 most highly enriched upregulated (gray) and downregulated (white) GO terms revealed changes in the DRG caused by amyotrophic lateral sclerosis (ALS).

3.3 Altered expression patterns of different dorsal root ganglia cell type-related genes differed between microgravity-exposed and SOD1^{G93A} mice

To determine the cell types that are sensitive to MG exposure, we identified DEGs within each group of cells in the DRG of AG- and MG-exposed mice (Avraham et al., 2020). We observed DEGs in various DRG cell type-related genes between MG- and AG-exposed mice (Table 1). DEGs were enriched in genes associated with immune and barrier cells, such as macrophages, T cells, endoneural cells, epineural cells, endothelial cells, and pericytes, rather than neurons and glia. These results suggest that MG altered transcriptional programs in the immune system and barrier function. Similarly, to determine which DRG cell type-related genes are affected by mutant SOD1 in the ALS group, we identified DEGs in each cell cluster-related gene between SOD1^{G93A} and WT mice at P30 and P120. The results revealed that gene expression was altered in most cell type-related genes of the DRG of SOD1^{G93A} mice at both stages, with more changes at P120 (Table 1). Remarkably, more differences in expression was observed in genes associated with all neurons, large to small diameter, of the DRG of SOD1^{G93A} mice (P30 large neurons, 0.84%; P30 medium/small, 1.12%; P120 large neurons, 2.86%; P120 medium/small, 2.83%) compared to MG-exposed mice (large, 0.38%; medium/small, 0.54%) (Table 1), which suggests that DRG neuron-related genes are more sensitive to changes caused by ALS than by gravity. Altogether, these results indicate that genes associated with various DRG cells are sensitive to and differentially affected by MG and ALS.

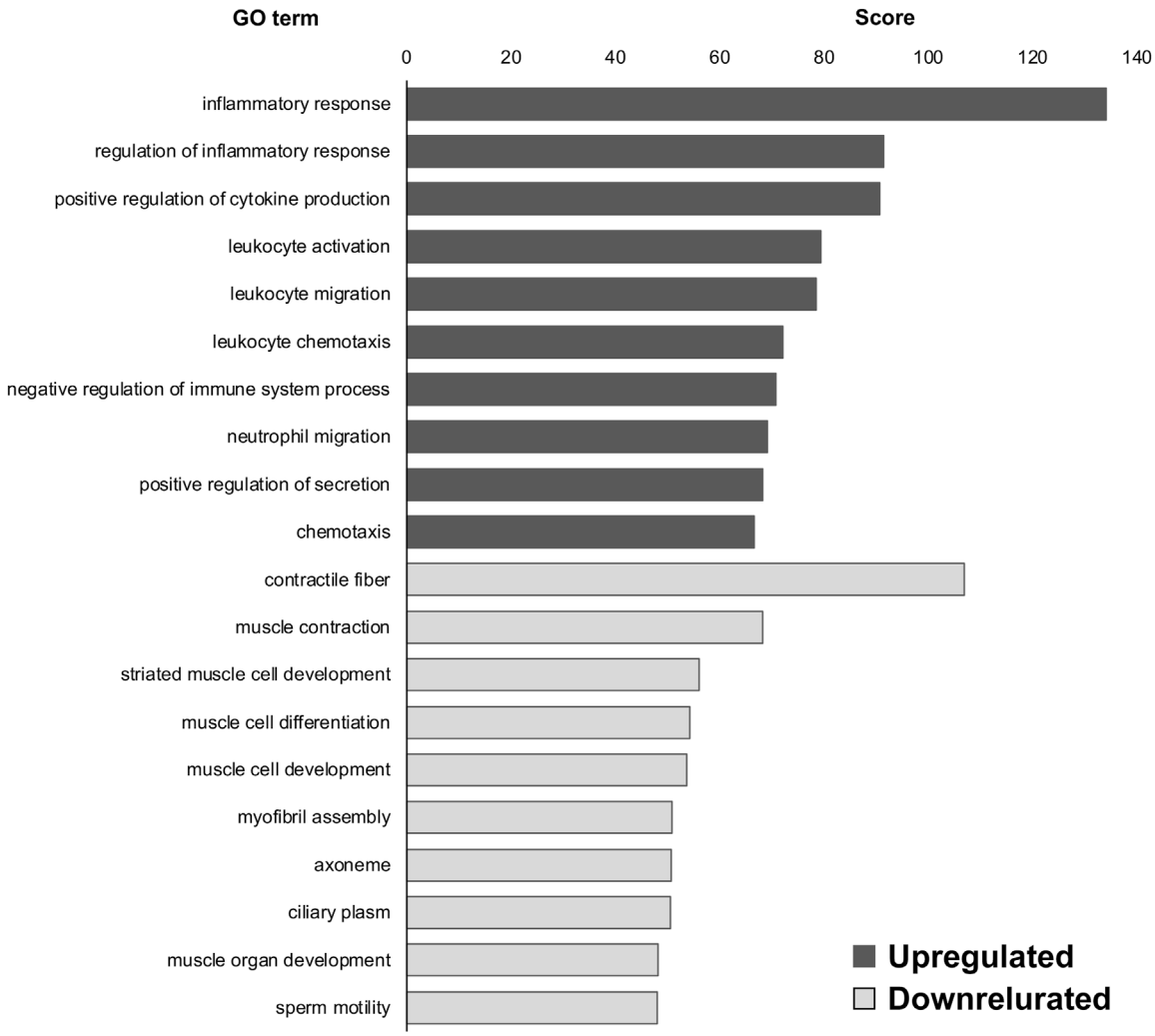

FIGURE 3
GO terms of DEGs in SOD1^{G93A} mice compared to WT mice at P120. Inflammatory response, regulation of inflammatory response, and positive regulation of cytokine production were the upregulated GO terms in the DRG of SOD1^{G93A} mice at P120 whereas contractile fiber, muscle contraction, and striated muscle cell development were the downregulated GO terms. Scores of the 10 most highly enriched upregulated (gray) and downregulated (white) GO terms revealed changes in the DRG caused by ALS.

3.4 Genes related to proprioceptive neurons in the dorsal root ganglia showed most expression changes in microgravity-exposed and SOD1^{G93A} mice

Our results show changes in neuron gene-expression levels in the DRG of mice subjected to MG (Table 1). Therefore, we examined the DEGs in various molecularly characterized neuronal populations in the DRG in our various models to further define the type of affected neurons (Li et al., 2016; Wu et al., 2021). We investigated the DRG of MG and ALS models and we observed more DEGs in putative proprioceptive neurons than in other neurons in MG-exposed and SOD1 ^{G93A} mice compared with their respective controls (Table 2). Additionally, a comparison between MG-exposed and SOD1^{G93A} mice showed that the latter had a higher number of DEGs in various DRG's putative neurons, notably, proprioceptive and nociceptive neurons (Table 2). These results show that sensory neurons, particularly proprioceptive neurons, change concomitantly with altered spinal motor neuron gene expression and muscle weakness.

3.5 Gene expression related to low-threshold mechanoreceptive and cold thermoreceptive neurons was altered in the dorsal root ganglia of microgravity-exposed and SOD1^{G93A} mice

The spinal cord receives convergent information from proprioceptive neurons innervating muscles and low-threshold mechanoreceptive (LTMR) neurons innervating the soles of feet and joints (Zholudeva et al., 2021), which are critical for adapting locomotion to changes in environment. To determine whether exposure to MG and ALS change the tactile system in the DRG, we analyzed LTMR neuron markers (Sharma et al., 2020). The levels of LTMR markers were elevated in both

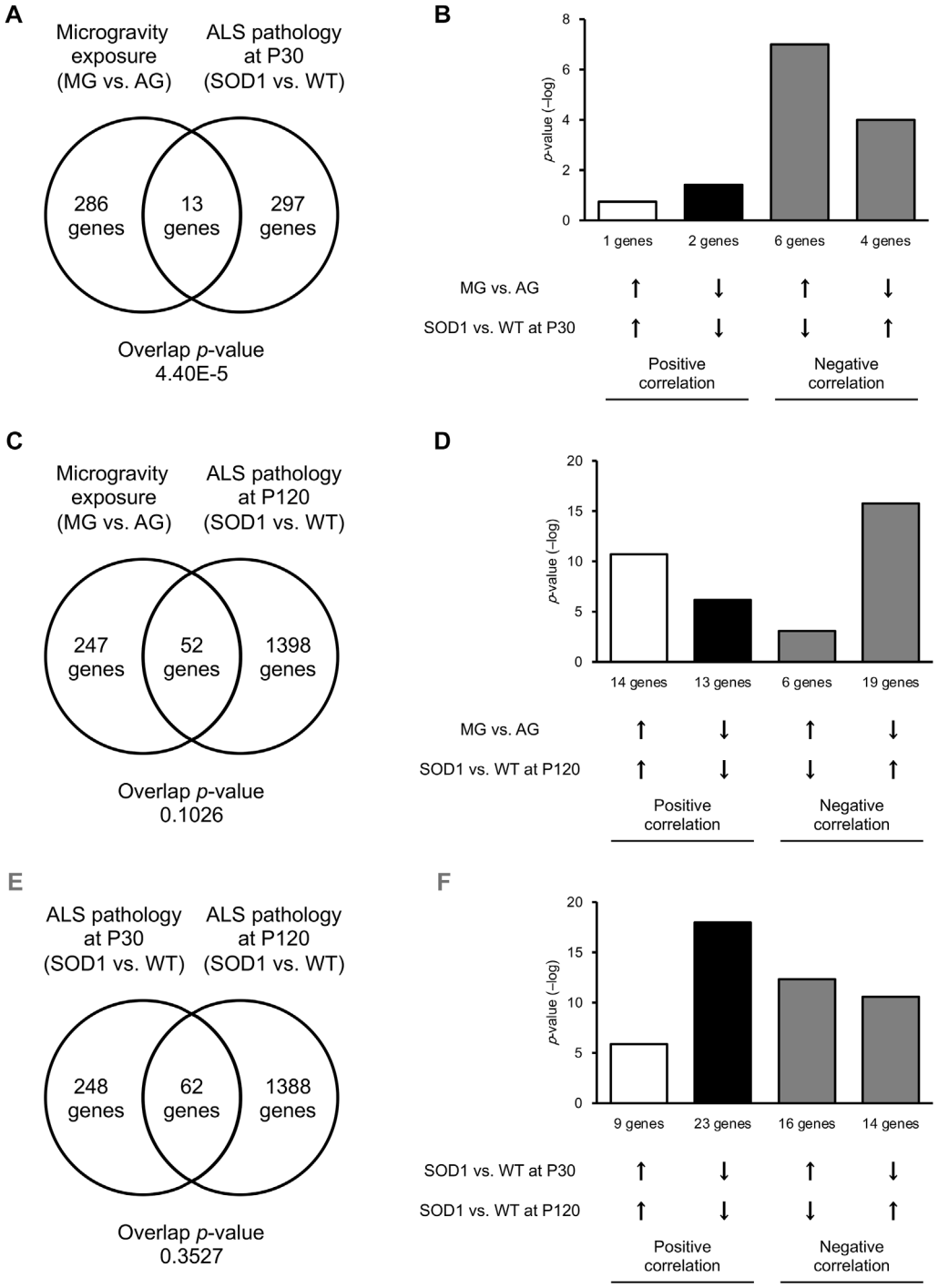

FIGURE 4
Common DEGs were increased in the DRG of MG-exposed and P120 SOD1^{G93A} mice. **(A–D)** DEG patterns after MG exposure compared with those with ALS in the DRG. Venn diagrams illustrate the overlap of DEGs in the DRG of MG-exposed mice (compared with AG-exposed mice) and SOD1^{G93A} mice (compared with WT mice) at P30 **(A)** and P120 **(C)**. Bar graphs illustrate the –log of overlapping *p*-values for upregulated (up arrows) or downregulated (down arrows) genes under each condition **(B,D)**. **(E,F)** Patterns of DEGs in SOD1^{G93A} DRG at an early stage compared with those of SOD1^{G93A} DRG at a late stage. Venn diagrams illustrate the overlap of DEGs in the DRG of SOD1^{G93A} mice (compared with WT mice) at P30 and P120 **(E)**. Bar graphs illustrate upregulated or downregulated genes under each condition **(F)**. *n* = 3 mice per group.

MG-exposed and SOD1^{G93A} mice compared with that respective controls (Table 3). Next, we analyzed cold thermoreceptive markers as altered cold sensations shown in MG-exposed human and patients with ALS (Dupuis et al., 2018; Buoite Stella et al., 2021). Remarkably, differential expression of cold thermoreceptor-related genes was observed in the DRG of MG-exposed and SOD1^{G93A} mice at P120 (Table 3). These results suggest that tactile and cold sensation systems are altered by exposure to MG and SOD1 mutation in mice.

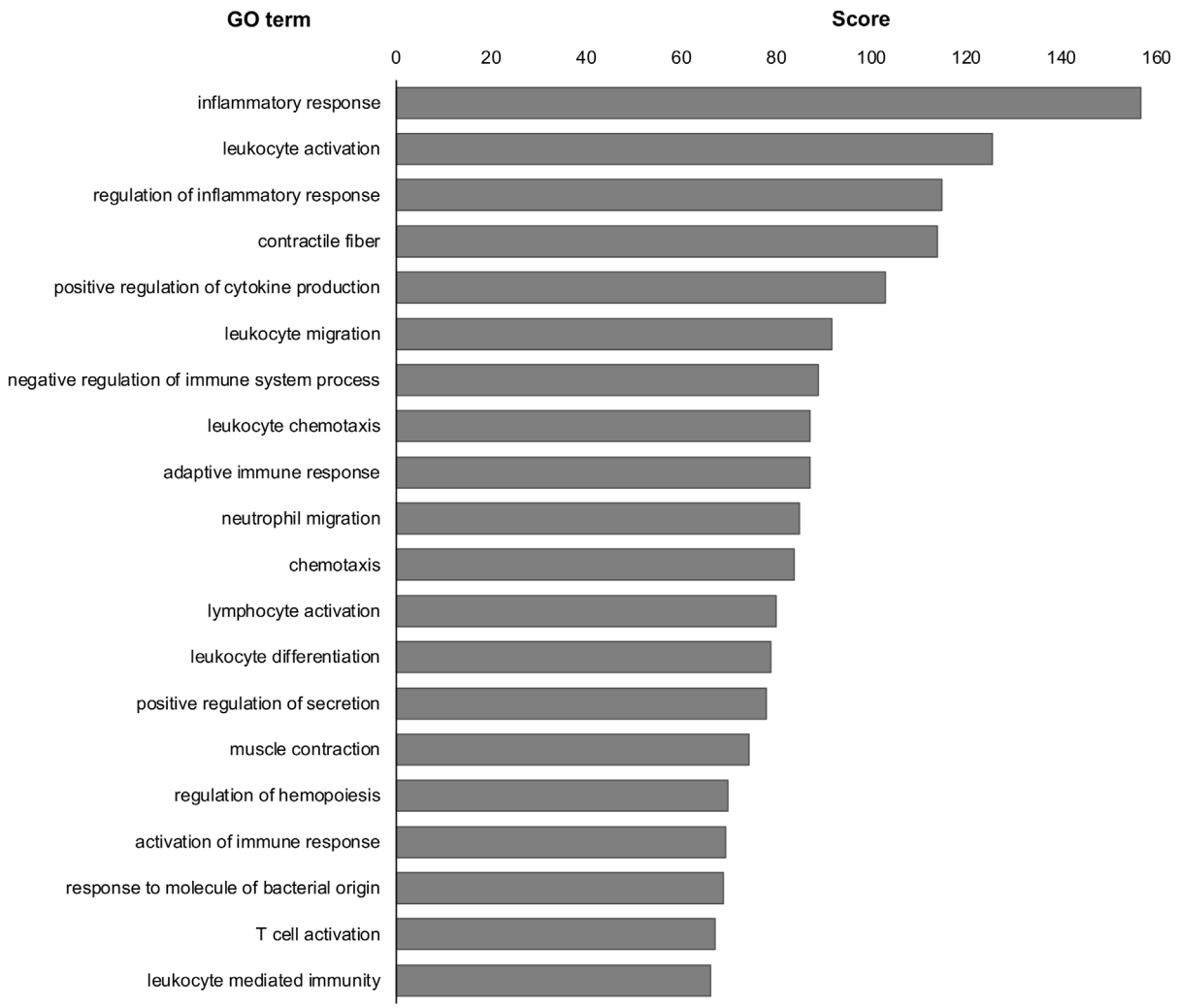

FIGURE 5
Common GO terms were analyzed in the DRG of MG-exposed and SOD1^{G93A} mice at P30 and P120. Inflammatory response, leukocyte activation, regulation of inflammatory response, contractile fiber, and positive regulation of cytokine production were common GO terms in the DRG of MG-exposed and SOD1^{G93A} mice at P30 and P120. Scores of the 20 most highly enriched GO terms revealed changes in the DRG caused by MG exposure and ALS.

3.6 Gene expression related to nociceptive neurons was more elevated in P120 SOD1^{G93A} mice than in microgravity-exposed and P30 SOD1^{G93A} mice

Altered pain sensitivity has been reported in MG-exposed humans and patients with ALS (Buoite Stella et al., 2021; Rubio et al., 2022). To confirm whether exposure to MG and ALS affect nociceptor levels, we used data on nociceptive neuron markers from previous DRG studies (Usoskin et al., 2015; Sharma et al., 2020; Huang et al., 2021). Expression of genes related to the calcitonin gene-related peptide (CGRP), a marker of peptidergic nociceptive DRG neurons (McCoy et al., 2013; Crawford and Caterina, 2020), were altered in the DRG of MG-exposed and SOD1^{G93A} mice (Table 3). The levels of nociceptor markers were elevated in SOD1^{G93A} mice at P120 (Table 4); however, these markers were rarely expressed in MG-exposed and SOD1^{G93A} mice at P30 (Table 4). Additionally, differential expression of skin- and lymph-node-innervating neuron-related genes was observed in the DRG of SOD1^{G93A} mice at P120 (Table 4), but few changes were detected in these neurons in MG-exposed and SOD1^{G93A} mice at P30 (Table 4), which indicates that nociceptors (innervating skin and lymph-node) are less sensitive to changes in MG and early stages of ALS.

3.7 Gene expression related to Imoonglia, macrophage, and satellite glial cells was affected in microgravity-exposed and SOD1^{G93A} mice

Immune and glial cell-related gene expression was altered in the spinal cord of MG-exposed and SOD1^{G93A} mice (Yoshikawa et al., 2022b). To decipher the various effects of exposure to MG and ALS pathology on immune and glial cells in the DRG microenvironment,

TABLE 1 Proportion of DEGs in putative DRG cell types of MG-exposed and SOD1^{G93A} mice at P30 and P120 (MG vs. AG-exposed mice, SOD1^{G93A} vs. WT mice).

Putative cell type	MG-exposed	P30 SOD1^{G93A}	P120 SOD1^{G93A}
Large neurons	0.38% (21/5459)	0.84% (46/5459)	2.86% (156/5459)
Medium/small neurons	0.54% (26/4838)	1.12% (54/4838)	2.83% (137/4838)
Mesenchymal endoneural cells	1.13% (25/2217)	0.72% (16/2217)	7.26% (161/2217)
Mesenchymal epineural cells	0.91% (18/1988)	0.45% (9/1988)	8.45% (168/1988)
Satellite glial cells	0.33% (5/1508)	0.27% (4/1508)	3.32% (50/1508)
Schwann cells	0.29% (4/1046)	0.29% (3/1046)	7.55% (79/1046)
Endothelial cells	0.97% (25/2579)	1.05% (27/2579)	5.51% (142/2579)
Pericytes	0.85% (19/2245)	0.67% (15/2245)	6.68% (150/2245)
Smooth muscle cells	1.07% (21/1955)	1.38% (27/1955)	7.42% (145/1955)
Macrophages	3.43% (80/2331)	0.77% (18/2331)	12.05% (281/2331)
T cells	3.17% (91/2874)	1.43% (41/2874)	9.64% (277/2874)

DEG, differentially expressed gene; DRG, dorsal root ganglia; MG, microgravity; AG, artificial gravity; SOD1, superoxide dismutase 1; WT, wild type; P, postnatal day. Cell types were defined as described by Avraham et al., 2020.

TABLE 2 Proportion of DEGs in putative DRG neuron classes of MG-exposed and SOD1^{G93A} mice at P30 and P120 (MG vs. AG-exposed mice, SOD1^{G93A} vs. WT mice).

Putative neuron class	MG-exposed	P30 SOD1^{G93A}	P120 SOD1^{G93A}
MHN	0.76% (1/131)	2.29% (3/131)	9.92% (13/131)
MHN (IS) 1	1.15% (1/87)	3.45% (3/87)	4.60% (4/87)
MHN (IS) 2	0% (0/361)	0.83% (3/361)	3.32% (12/361)
MHN (MI, IS)	0.35% (1/288)	0.69% (2/288)	11.11% (32/288)
MHN (MS), proprioceptors	2.99% (2/67)	0% (0/67)	29.85% (20/67)
MN	0.74% (1/135)	1.48% (2/135)	5.19% (7/135)
MR	0.86% (3/348)	0.86% (3/348)	5.46% (19/348)
C-LTMR	0% (0/126)	0.79% (1/126)	4.76% (6/126)
Satellite glial cells	0.99% (3/303)	0.33% (1/303)	4.29% (13/303)
Blood cells	0% (0/42)	7.14% (3/42)	7.14% (3/42)
Proprioceptive neurons			
Ia 1	0% (0/151)	0.66% (1/151)	11.92% (18/151)
Ia 2	0.50% (2/398)	1.76% (7/398)	9.80% (39/398)
Ia 3	0.72% (4/554)	0.54% (3/554)	7.22% (40/554)
Ib	0.48% (2/421)	0.48% (2/421)	10.45% (44/421)
II 1	0% (0/262)	0.76% (2/262)	9.54% (25/262)
II 2	0.64% (1/156)	1.92% (3/156)	10.90% (17/156)
II 3	0.57% (3/529)	0.76% (4/529)	6.62% (35/529)
II 4	0.34% (2/582)	0.86% (5/582)	5.67% (33/582)

DEG, differentially expressed gene; DRG, dorsal root ganglia; MG, microgravity; AG, artificial gravity; SOD1, superoxide dismutase 1; WT, wild type; P, postnatal day; MHN, mechanoheat nociceptor; IS, itch sensitive; MS, mechanically sensitive; MI, mechanically insensitive; MN, mechanical nociceptor; MR, mechanoreceptor; LTMR, low-threshold mechanoreceptor. Cell types were defined as described by Li et al., 2016 and Wu et al., 2021.

we examined Imoonglia expressing macrophage and glial markers, macrophage, and SGC-related genes in the DRG of MG-exposed and SOD1^{G93A} mice (Avraham et al., 2021; Feng et al., 2023). The effects of MG were stronger on Imoonglia and macrophage genes than on SGC genes (Table 5). DEGs in Imoonglia, macrophages, and various putative SGC cell types were detected in the DRG of P120 SOD1^{G93A} mice, and slight changes were observed in these cells in P30 SOD1^{G93A} mice (Table 5). These results indicate that exposure to MG and ALS stimulates gene expression of immune and glial cells in the DRG.

TABLE 3 Proportion of DEGs in DRG sensory neuron subtypes of MG-exposed and SOD1^{G93A} mice at P30 and P120 (MG vs. AG-exposed mice, SOD1^{G93A} vs. WT mice).

Putative neuron type	MG-exposed	P30 SOD1^{G93A}	P120 SOD1^{G93A}
Aβ field-LTMR	4.00% (2/50)	4.00% (2/50)	16.00% (8/50)
Aβ RA-LTMR	6.00% (3/50)	2.00% (1/50)	26.00% (13/50)
Aδ-LTMR	4.00% (2/50)	4.00% (2/50)	20.00% (10/50)
C-LTMR	8.00% (4/50)	0% (0/50)	20.00% (10/50)
CGRP-α	6.00% (3/50)	4.00% (2/50)	10.00% (5/50)
CGRP-ε	2.04% (1/49)	2.04% (1/49)	12.24% (6/49)
CGRP-γ	6.12% (3/49)	0% (0/49)	12.24% (6/49)
CGRP-η	4.00% (2/50)	0% (0/50)	14.00% (7/50)
CGRP-θ	4.17% (2/48)	2.08% (1/48)	10.41% (5/48)
CGRP-ζ	6.12% (3/49)	4.08% (2/49)	14.29% (7/49)
Cold thermoreceptors	4.26% (2/47)	0% (0/47)	12.77% (6/47)
Polymodal nociceptors	0% (0/49)	2.04% (1/49)	6.12% (3/49)
Pruriceptors	4.00% (2/50)	0% (0/50)	24.00% (12/50)
Proprioceptors	0% (0/50)	2.00% (1/50)	44.00% (22/50)

DEG, differentially expressed gene; DRG, dorsal root ganglia; MG, microgravity; AG, artificial gravity; SOD1, superoxide dismutase 1; WT, wild type; P, postnatal day; LTMR, low-threshold mechanoreceptor; CGRP, calcitonin gene-related peptide. Cell types were defined as described by Sharma et al., 2020.

TABLE 4 Proportion of DEGs in putative DRG neuron types of MG-exposed and SOD1^{G93A} mice at P30 and P120 (MG vs. AG-exposed mice, SOD1^{G93A} vs. WT mice).

Putative DRG neuron type	MG-exposed	P30 SOD1^{G93A}	P120 SOD1^{G93A}
Non-peptidergic nociceptors 1	0.86% (3/348)	1.15% (4/348)	13.22% (46/348)
Non-peptidergic nociceptors 2	0.33% (1/303)	0.66% (2/303)	9.24% (28/303)
Non-peptidergic nociceptors 3	0% (0/206)	0.97% (2/206)	9.71% (20/206)
Peptidergic nociceptors 1	0.56% (2/358)	1.40% (5/358)	12.85% (46/358)
Peptidergic nociceptors 2	0.75% (2/265)	0.75% (2/265)	9.43% (25/265)
LTMR 1	0% (0/242)	0.83% (2/242)	9.50% (23/242)
LTMR 2	0.65% (2/310)	0.65% (2/310)	14.52% (45/310)
LTMR 3	0.90% (2/223)	0.45% (1/223)	10.76% (24/223)
C-LTMR	0.81% (3/369)	0.81% (3/369)	13.82% (51/369)
Proprioceptor 1	0% (0/254)	0.39% (1/254)	15.35% (39/254)
Proprioceptor 2	0.43% (1/233)	0.43% (1/233)	14.59% (34/233)
Lymph nodes-innervating	0.99% (1/101)	1.98% (2/101)	8.91% (9/101)
Skin-innervating	0% (0/156)	0.64% (1/156)	6.41% (10/156)

DEG, differentially expressed gene; DRG, dorsal root ganglia; MG, microgravity; AG, artificial gravity; SOD1, superoxide dismutase 1; WT, wild type; P, postnatal day; LTMR, low-threshold mechanoreceptor. Cell types were defined as described by Usoskin et al., 2015 and Huang et al., 2021.

3.8 Injury-induced gene expression in dorsal root ganglia was more affected in P120 SOD1^{G93A} mice than microgravity-exposed and P30 SOD1^{G93A} mice

The expression of genes related to axon injury was altered in the DRG of MG-exposed and SOD1^{G93A} mice (Supplementary Tables S1–S3). To assess whether exposure to MG or ALS induces axonal damage, we compared altered gene expression in the DRG of sciatic nerve transected mice with that in the DRG of MG-exposed and SOD1^{G93A} mice (Renthal et al., 2020). Expression of injury-induced DRG neuron-related genes increased in the DRG of SOD1^{G93A} mice at P120 but not that of MG-exposed and P30 SOD1^{G93A} mice compared with their respective controls (Table 6), which suggest that axonal injury does not occur or is less prominent in MG-exposed and P30 SOD1^{G93A} mice.

TABLE 5 Proportion of DEGs in putative Imoonglia, macrophages, and satellite glial cells in the DRG of MG-exposed and SOD1^{G93A} mice at P30 and P120 (MG vs. AG-exposed mice, SOD1^{G93A} vs. WT mice).

Putative cell type	MG-exposed	P30 SOD1^{G93A}	P120 SOD1^{G93A}
Imoonglia	5.74% (63/1097)	1.09% (12/1097)	16.96% (186/1097)
Macrophages	3.81% (94/2469)	1.50% (37/2469)	13.28% (328/2469)
Satellite glial cells			
Cluster 1	1.40% (7/500)	2.00% (10/500)	8.00% (40/500)
Cluster 2	3.08% (10/325)	2.46% (8/325)	15.69% (51/325)
Cluster 3	0.60% (3/500)	0.20% (1/500)	9.00% (45/500)
Cluster 4	0.20% (1/500)	0.60% (3/500)	12.40% (62/500)
Astrocyte	1.20% (6/500)	1.40% (7/500)	14.00% (70/500)
Non-myelinated Schwann cells	0% (0/80)	0% (0/80)	13.75% (11/80)
Myelinated Schwann cells	0% (0/99)	1.01% (1/99)	17.17% (17/99)

DEG, differentially expressed gene; DRG, dorsal root ganglia; MG, microgravity; AG, artificial gravity; SOD1, superoxide dismutase 1; WT, wild type; P, postnatal day. Cell types were defined as described by Avraham et al., 2021.

TABLE 6 Proportion of differentially expressed axonal injury-neuronal genes and proportion of differentially expressed endothelial cells, pericytes, Schwann cells, macrophages, and satellite glial cells genes after dorsal root crush, spinal cord injury, and sciatic nerve crush in the DRG of MG-exposed and SOD1^{G93A} mice at P30 and P120 (MG vs. AG-exposed mice, SOD1^{G93A} vs. WT mice).

Putative neuronal and non-neuronal cell type	MG-exposed	P30 SOD1^{G93A}	P120 SOD1^{G93A}
Injury-induced neuronal genes	0.76% (4/524)	0.57% (3/524)	10.69% (56/524)
Dorsal root crush			
Endothelial cells	2.70% (17/630)	0.63% (4/630)	15.24% (96/630)
Pericytes	2.64% (15/568)	0.70% (4/568)	14.79% (84/568)
Schwann cells	2.76% (19/689)	0.73% (5/689)	15.82% (109/689)
Macrophages	3.04% (14/460)	1.52% (7/460)	15.43% (71/460)
Satellite glial cells	0.57% (1/174)	1.15% (2/174)	18.39% (32/174)
Spinal cord injury			
Endothelial cells	4.33% (10/231)	0% (0/231)	18.61% (43/231)
Pericytes	3.91% (10/256)	1.56% (4/256)	15.23% (39/256)
Schwann cells	2.41% (6/249)	1.20% (3/249)	17.27% (43/249)
Macrophages	2.67% (2/75)	0% (0/75)	24.00% (18/75)
Satellite glial cells	1.54% (1/65)	0% (0/65)	30.77% (20/65)
Sciatic nerve crush			
Endothelial cell	2.35% (30/1276)	0.31% (4/1276)	8.62% (110/1276)
Pericytes	2.19% (21/957)	0.52% (5/957)	12.64% (121/957)
Schwann cells	1.97% (25/1271)	0.63% (8/1271)	10.62% (135/1271)
Macrophages	3.08% (21/682)	1.17% (8/682)	15.54% (106/682)
Satellite glial cells	0.63% (3/479)	0.84% (4/479)	8.35% (40/479)

DEG, differentially expressed gene; DRG, dorsal root ganglia; MG, microgravity; AG, artificial gravity; SOD1, superoxide dismutase 1; WT, wild type; P, postnatal day. Cell types were defined as described by Renthal et al., 2020 and Avraham et al., 2021.

3.9 Expression of genes related to non-neuronal cells after central and peripheral axonal injuries was altered in P120 SOD1^{G93A} mice but not in microgravity-exposed and P30 SOD1^{G93A} mice

To compare the effects of exposure to MG and ALS on non-neuronal cells in the DRG, we examined the expression of genes related to endothelial cells, Schwann cells, pericytes, macrophages, and SGCs of dorsal root crushed, spinal cord injured, and sciatic nerve crushed mice (Avraham et al., 2021). Compared to their control counterparts, an increase in the DEGs related to injury was observed in SOD1^{G93A} mice at P120, but not at P30, and a slight increase was also observed in MG-exposed mice compared to the AG controls (Table 6). These results indicate that P120 ALS affects expression of non-neuronal cell-related genes in the DRG associated with spinal cord and nerve injuries and that MG has slighter effects compared to P120 SOD1^{G93A} mice.

4 Discussion

Exposure to MG and ALS are associated with changes in various physiological functions, which leads to alterations in the cardiovascular, musculoskeletal, immune, membrane transporter, and motor systems. Several studies have demonstrated that defects in the sensory components of the sensorimotor system contribute to motor neuron dysfunction in the pathogenic process of motor neuron diseases, such as spinal muscular atrophy (Shorrock et al., 2019), and it has been suggested that the sensory system may be affected just like the motor system (Rubio et al., 2022). Here, we investigated and compared the effects of exposure to MG on the DRG with an ALS mouse model expressing the mutant SOD1^{G93A}, which exhibits similar motor deficits. SOD1^{G93A} mice show neuromuscular junction denervation, mitochondrial abnormalities in spinal motor neurons, and altered spinal neurovascular units at P30 (Vinsant et al., 2013a; Vinsant et al., 2013b; Yoshikawa et al., 2022a) and numerous pathological changes, including spinal motor neuron loss at P120 (Vinsant et al., 2013a). By analyzing the characteristics of MG- and mutant SOD1-induced degeneration, we aimed to obtain new insights into neurodegenerative diseases, which could lead to new treatments, targeting the DRG.

In this study, we hypothesized that MG and ALS would result in different pathophysiological adaptations. To this end, we investigated the effects of exposure to MG and mutant SOD1 on gene expression related to various cell types in the mouse DRG. The results showed that the direction of several common GO terms was different in the DRG of MG and ALS mice. For example, the GO term inflammatory response was downregulated in the DRG of MG-exposed and P30 SOD1^{G93A} mice, while upregulated in SOD1^{G93A} mice at P120. Furthermore, common DEGs between the DRG of MG-exposed and ALS mice were increased in the late stages of ALS. Several DEGs were observed in genes related to putative DRG cell types in both experimental mouse models. Several types of cells associated with the immune system and barrier formation are affected by exposure to MG. Differential expression alterations were observed in whole range of neurons of the DRG of SOD1^{G93A} mice compared with MG-exposed mice. Several ALS-causing genes have been linked to sensory dysfunctions, and mutant SOD1 and TDP-43 have been reported to be associated with sensory abnormalities prior to motor neuron death, with mitochondrial damage (Guo et al., 2009; Tao et al., 2018). Altered gene expression was observed in the DRG of SOD1^{G93A} mice as early as P30; however, SOD1-associated ALS is only one of many forms of ALS, and we need to expand to other forms of ALS.

The expression of several SLC family-related genes in the DRG of MG-exposed and SOD1^{G93A} mice at P30 and P120 was altered. Multiple SLCs are expressed in the DRG cells and located in the plasma membranes of DRG neurons (Sprowl et al., 2013; Yi et al., 2021). SLC genes have been identified in the brain, particularly in barrier cells (Ayka and Şehirli, 2020; Hu et al., 2020; Kumar et al., 2022). Several studies have indicated the neuroprotective role of SLCs in neurodegeneration-inducing conditions, such as hypoxia and ischemia, and diseases such as Alzheimer's and Parkinson's disease, through reducing redox signaling (Ayka and Şehirli, 2020; Nguyen et al., 2021; Kumar et al., 2022). DEGs of the Slc6 family, neurotransmitter transporters, and the Slc25a family, mitochondrial carriers, were altered in SOD1^{G93A} mice at P30 and P120, which deserves consideration (Hu et al., 2020; Kumar et al., 2022). However, SLCs in the DRG have not yet been well evaluated and remains to be determined.

In this study, the expression of proprioceptive neuron markers decreased in the DRG of MG-exposed and SOD1^{G93A} mice at P120, whereas it did not change at P30. Exposure to MG induced changes in the activity of oxidative enzymes in large-diameter DRG neurons (Nagatomo et al., 2014). Previous studies suggested that exposure to MG and ALS alter in large-diameter, putative proprioceptive, DRG neurons and axons, resulting in motor system dysfunction (Nagatomo et al., 2014; Sábado et al., 2014; Rubio et al., 2022). Additionally, large proprioceptive neurons were shown to undergo a degenerative process involving the inflammatory recruitment of macrophages (Sábado et al., 2014), and proprioceptive synapses, muscle spindle afferent inputs to motor neurons, were reduced on the motor neurons in the SOD1^{G93A} spinal cord (Schütz, 2005; Vaughan et al., 2015). Motor neuron survival increased in SOD1^{G93A}; Egr3^{KO} double mutant mice (proprioception altered in SOD1^{G93A} mice), suggesting that proprioceptive sensory activity contributes to motor neuron degeneration (Lalancette-Hebert et al., 2016). These results suggest that changes in genes related to proprioceptive neurons may contribute to the motor dysfunction associated with exposure to MG and the late stage of ALS and may reflect muscle weakness.

Expression of LTMR-related genes was also altered in the DRG of MG-exposed and SOD1^{G93A} mice. Tactile sensory inputs are required to generate appropriate movements (Paixão et al., 2019), and cutaneous pathways contribute to corrective movements during locomotion, via networks in the spinal cord that integrate tactile and proprioceptive information (Zholudeva et al., 2021). In microgravity, tactile sense is affected, as astronauts feel less (or no) pressure on their feet, leading to sensory deprivation (Hupfeld et al., 2021). Therefore, changes in mechanoreceptors may cause the motor dysfunction associated with exposure to MG and ALS. Moreover, expression of cold thermoreceptor-related genes was altered in the DRG of MG-exposed and SOD1^{G93A} mice. Additionally, cold-cutaneous stimulation modulates motor neuron activity (Tamura et al., 2019). However, whether altered cold thermoreceptors potentially contribute to the motor deficits caused by exposure to MG and ALS remains to be determined.

Given that skin alterations have been reported following exposure to MG and ALS progression (Pampalakis et al., 2019; Radstake et al., 2022), but that changes in skin- and lymph-node-innervating neuron-related genes were mild in MG-exposed and

SOD1^{G93A} mice at P30, we conclude that effects of inflammation on nociceptive neurons in the DRG caused by MG exposure and early ALS are minimal. Additionally, expression of nociceptor-related genes was mildly altered in the DRG of MG-exposed mice, whereas expression of CGRP-related genes was altered in the DRG of MG-exposed mice. CGRP-positive neurons are, in addition to nociceptors, associated with high-threshold mechanosensory and cold sensations (McCoy et al., 2013; Kuehn et al., 2019; Crawford and Caterina, 2020). Therefore, alterations in the CGRP-positive neurons may not be limited to nociceptive functions. In the DRG of SOD1^{G93A} mice at P120, the expression of nociceptors and skin- and lymph-node-innervating neuron-related genes was altered, showing increased cytokine and axon injury markers, suggesting that DRG cells are affected by inflammation and axonal damage upon disease progression.

The expression of axonal injury-induced factors is altered in the DRG of MG-exposed and SOD1^{G93A} mice. Long-term exposure to microgravity and ALS have been shown to induce multi-organ damage, including the brain, spinal cord, and DRG dysfunction (Guo et al., 2009; Vinsant et al., 2013a; Vinsant et al., 2013b; Holley et al., 2022; Li et al., 2022; Mhatre et al., 2022; Rubio et al., 2022; Yoshikawa et al., 2022b). Therefore, we compared the DRG of MG-exposed and SOD1^{G93A} mice with that of animals subjected to different injury conditions (Avraham et al., 2021). The expression of *Atf3*, which is increased in DRG neurons in ALS mouse model (SOD1^{G93A} and TDP43^{A315T} mice; Vaughan et al., 2018), and SGC-related genes, which is increased in response to peripheral nerve injury (Avraham et al., 2021), changed in the DRG of SOD1^{G93A} mice at P120 but not in MG-exposed and P30 SOD1^{G93A} mice, which may reflect DRG neuron and axon damage in P120 SOD1^{G93A} mice (Vaughan et al., 2018). ATF3 is known to be a stress-responsive molecular hub for a variety of cell types (Ku and Cheng, 2020). While ATF3 expression may indicate axonal damage, neurons without axonal damage but with metabolic stress, or by SGCs, or by resident or invading immune cells may also express ATF3 (Hunt et al., 2012). Previous study indicates that proprioceptive neurons, in addition to all other neurons in the DRG, resist degeneration during the early stages of ALS (Vaughan et al., 2015). Furthermore, the expression of Imoonglia-related genes was altered in the DRG of MG-exposed and P120 SOD1^{G93A} mice. Imoonglia in the DRG activate following both peripheral and central injuries (Avraham et al., 2021). These results suggest that the DRG microenvironment in MG-exposed and SOD1^{G93A} mice is different, and exposure to MG- and P30 ALS-induced neuronal damage is mild, and the genes may not respond.

The expression of genes related to endothelial cells, pericytes, mesenchymal endoneural cells, and mesenchymal epineural cells was altered in the DRG of MG-exposed and SOD1^{G93A} mice. These cells are related to physical barriers, including the blood–nerve barrier, which protects peripheral nerves from external influencing factors and are altered following peripheral nerve injury (Liu et al., 2018). Additionally, injury-induced gene expression related to endothelia cells and pericytes was observed in the DRG of MG-exposed and SOD1^{G93A} mice. Therefore, alterations to these cells may influence the barrier integrity and, consequently, peripheral nervous system injury.

In conclusion, we describe the effects of exposure to MG and ALS on the DRG. Our study supports the involvement of the sensory system in exposure to microgravity and in the SOD1 transgenic mouse model of ALS. We first determined the DEGs in the DRG of MG-exposed (compared with AG-exposed) and early and late stages of SOD1^{G93A} (compared with WT) mice. Our results revealed changes in various neuronal and non-neuronal cell-related gene expression in the DRG in response to exposure to MG or ALS, especially proprioceptive neurons, mechanoreceptive neurons, glial cells, immune cells, and barrier cells. A better understanding of the role of the sensory system, in response to exposure to MG and ALS, may provide opportunities to elucidate the determinants of the different vulnerability patterns between the MG-exposed and SOD1 mice, which could allow the identification of new therapeutic targets for patients with motor disturbances.

Data availability statement

The datasets generated for this study are available from the corresponding author upon reasonable request. RNA-seq data generated for this study can be found in the DNA Databank of Japan (DDBJ) database (https://www.ddbj.nig.ac.jp/; accession numbers DRA015057, DRA015058 and DRA015059).

Ethics statement

The animal study was reviewed and approved by The Institutional Animal Care and Use Committee of the University of Tsukuba, JAXA, Explore Biolabs, NASA, and Nihon University School of Medicine.

Author contributions

MY designed and performed the experiments, analyzed and interpreted the data, and wrote the manuscript. MM and HO collaborated on the experiments and the data analysis. CI, HL, and TK performed sample preparation. MM collaborated the data collection. ST, DS, MS, MU, and SA supervised the experiments. TS designed and supervised the experiments. All authors contributed to the article and approved the submitted version.

Funding

This work was supported by a Grant-in-Aid (14YPTK-005512) from JAXA (TS), a Grant-in-Aid for Scientific Research (JP18K06510) from the Ministry of Education, Culture, Sports, Science, and Technology (MEXT) of Japan (MY), and Nihon University School of Medicine 50th Anniversary Fund Research Grant (2016) (MY, MM, and HO).

Acknowledgments

We sincerely thank the support of CeresBioscience (Saitama, Japan) for the bioinformatic analysis. We also thank Akane Yumoto of the

Japan Aerospace Exploration Agency (JAXA) and Hiromi Suzuki of the Japan Space Forum for coordinating the study and Naoko Murakami and Rika Oshima of the Advanced Engineering Services Co., Ltd. for their assistance with animal care. We thank the personnel of JAXA and the NASA Johnson Space Center and Kennedy Space Center for carrying our animal models on their spaceflight. We also thank Enago (https://www.enago.jp) and Editage (https://www.editage.jp/) for editing a draft of this manuscript.

Conflict of interest

The authors declare that the research was conducted in the absence of any commercial or financial relationships that could be construed as a potential conflict of interest.

Publisher's note

Supplementary material

The Supplementary Material for this article can be found online at: https://www.frontiersin.org/articles/10.3389/frspt.2023.1162268/full#supplementary-material

References

Avraham, O., Deng, P. Y., Jones, S., Kuruvilla, R., Semenkovich, C. F., Klyachko, V. A., et al. (2020). Satellite glial cells promote regenerative growth in sensory neurons. *Nat. Commun.* 11, 4891. doi:10.1038/s41467-020-18642-y

Avraham, O., Feng, R., Ewan, E. E., Rustenhoven, J., Zhao, G., and Cavalli, V. (2021). Profiling sensory neuron microenvironment after peripheral and central axon injury reveals key pathways for neural repair. *eLife* 10, e68457. doi:10.7554/eLife.68457

Ayka, A., and Şehirli, A. Ö. (2020). The role of the SLC transporters protein in the neurodegenerative disorders. *Clin. Psychopharmacol. Neurosci.* 18, 174–187. doi:10.9758/cpn.2020.18.2.174

Buoite Stella, A., Ajčević, M., Furlanis, G., and Manganotti, P. (2021). Neurophysiological adaptations to spaceflight and simulated microgravity. *Clin. Neurophysiol.* 132, 498–504. doi:10.1016/j.clinph.2020.11.033

Carriot, J., Mackrous, I., and Cullen, K. E. (2021). Challenges to the vestibular system in space: How the brain responds and adapts to microgravity. *Front. Neural Circuits.* 15, 760313. doi:10.3389/fncir.2021.760313

Chia, R., Chiò, A., and Traynor, B. J. (2018). Novel genes associated with amyotrophic lateral sclerosis: Diagnostic and clinical implications. *Lancet Neurol.* 17, 94–102. doi:10.1016/S1474-4422(17)30401-5

Clément, G., and Wood, S. J. (2014). Rocking or rolling-perception of ambiguous motion after returning from space. *PLOS ONE* 9, e111107. doi:10.1371/journal.pone.0111107

Crawford, L. K., and Caterina, M. J. (2020). Functional anatomy of the sensory nervous system: Updates from the neuroscience bench. *Toxicol. Pathol.* 48, 174–189. doi:10.1177/0192623319869011

Dupuis, L., Petersen, Å., and Weydt, P. (2018). Thermoregulation in amyotrophic lateral sclerosis. *Handb. Clin. Neurol.* 157, 749–760. doi:10.1016/B978-0-444-64074-1.00046-X

Elcombe, C. S., Monteiro, A., Elcombe, M. R., Ghasemzadeh-Hasankolaei, M., Sinclair, K. D., Lea, R., et al. (2022). Developmental exposure to real-life environmental chemical mixture programs a testicular dysgenesis syndrome-like phenotype in prepubertal lambs. *Environ. Toxicol. Pharmacol.* 94, 103913. doi:10.1016/j.etap.2022.103913

Feng, R., Muraleedharan Saraswathy, V., Mokalled, M. H., and Cavalli, V. (2023). Self-renewing macrophages in dorsal root ganglia contribute to promote nerve regeneration. *Proc. Natl. Acad. Sci. USA.* 120, e2215906120. doi:10.1073/pnas.2215906120

Gunes, Z. I., Kan, V. W. Y., Ye, X., and Liebscher, S. (2020). Exciting complexity: The role of motor circuit elements in ALS pathophysiology. *Front. Neurosci.* 14, 573. doi:10.3389/fnins.2020.00573

Guo, Y. S., Wu, D. X., Wu, H. R., Wu, S. Y., Yang, C., Li, B., et al. (2009). Sensory involvement in the SOD1-G93A mouse model of amyotrophic lateral sclerosis. *Exp. Mol. Med.* 41, 140–150. doi:10.3858/emm.2009.41.3.017

Gurney, M. E., Pu, H., Chiu, A. Y., Dal Canto, M. C., Polchow, C. Y., Alexander, D. D., et al. (1994). Motor neuron degeneration in mice that express a human Cu,Zn superoxide dismutase mutation. *Science* 264, 1772–1775. doi:10.1126/science.8209258

Holley, J. M., Stanbouly, S., Pecaut, M. J., Willey, J. S., Delp, M., and Mao, X. W. (2022). Characterization of gene expression profiles in the mouse brain after 35 days of spaceflight mission. *npj Microgravity* 8, 35. doi:10.1038/s41526-022-00217-4

Hu, C., Tao, L., Cao, X., and Chen, L. (2020). The solute carrier transporters and the brain: Physiological and pharmacological implications. *Asian J. Pharm. Sci.* 15, 131–144. doi:10.1016/j.ajps.2019.09.002

Huang, S., Ziegler, C. G. K., Austin, J., Mannoun, N., Vukovic, M., Ordovas-Montanes, J., et al. (2021). Lymph nodes are innervated by a unique population of sensory neurons with immunomodulatory potential. *Cell* 184, 441–459.e25. doi:10.1016/j.cell.2020.11.028

Hunt, D., Raivich, G., and Anderson, P. N. (2012). Activating transcription factor 3 and the nervous system. *Front. Mol. Neurosci.* 5, 7. doi:10.3389/fnmol.2012.00007

Hupfeld, K. E., McGregor, H. R., Reuter-Lorenz, P. A., and Seidler, R. D. (2021). Microgravity effects on the human brain and behavior: Dysfunction and adaptive plasticity. *Neurosci. Biobehav. Rev.* 122, 176–189. doi:10.1016/j.neubiorev.2020.11.017

Iglesias, C., Sangari, S., El Mendili, M. M., Benali, H., Marchand-Pauvert, V., and Pradat, P. F. (2015). Electrophysiological and spinal imaging evidences for sensory dysfunction in amyotrophic lateral sclerosis. *BMJ Open* 5, e007659. doi:10.1136/bmjopen-2015-007659

Ikeda, H., Muratani, M., Hidema, J., Hada, M., Fujiwara, K., Souda, H., et al. (2019). Expression profile of cell cycle-related genes in human fibroblasts exposed simultaneously to radiation and simulated microgravity. *Int. J. Mol. Sci.* 20, 4791. doi:10.3390/ijms20194791

Kim, G., Gautier, O., Tassoni-Tsuchida, E., Ma, X. R., and Gitler, A. D. (2020). ALS genetics: Gains, losses, and implications for future therapies. *Neuron* 108, 822–842. doi:10.1016/j.neuron.2020.08.022

Ku, H. C., and Cheng, C. F. (2020). Master regulator activating transcription factor 3 (ATF3) in metabolic homeostasis and cancer. *Front. Endocrinol. (Lausanne).* 11, 556. doi:10.3389/fendo.2020.00556

Kuehn, E. D., Meltzer, S., Abraira, V. E., Ho, C. Y., and Ginty, D. D. (2019). Tiling and somatotopic alignment of mammalian low-threshold mechanoreceptors. *Proc. Natl. Acad. Sci. USA.* 116, 9168–9177. doi:10.1073/pnas.1901378116

Kumar, R., Amruthanjali, T., Singothu, S., Singh, S. B., and Bhandari, V. (2022). Uncoupling proteins as a therapeutic target for the development of new era drugs against neurodegenerative disorder. *Biomed. Pharmacother.* 147, 112656. doi:10.1016/j.biopha.2022.112656

Lalancette-Hebert, M., Sharma, A., Lyashchenko, A. K., and Shneider, N. A. (2016). Gamma motor neurons survive and exacerbate alpha motor neuron degeneration in ALS. *Proc. Natl. Acad. Sci. U. S. A.* 113, E8316–E8325. doi:10.1073/pnas.1605210113

Latif, S., and Kang, Y. S. (2022). Blood-brain barrier solute carrier transporters and motor neuron disease. *Pharmaceutics* 14, 2167. doi:10.3390/pharmaceutics14102167

Li, C. L., Li, K. C., Wu, D., Chen, Y., Luo, H., Zhao, J. R., et al. (2016). Somatosensory neuron types identified by high-coverage single-cell RNA-sequencing and functional heterogeneity. *Cell Res.* 26, 83–102. doi:10.1038/cr.2015.149

Li, Y., Zhang, H., Ren, N., Chen, C., Qi, P., Zhou, F., et al. (2022). Oral pyruvate effects on dorsal root ganglia in simulated weightlessness rats. *J. Neurol. Res.* 12, 9–20. doi:10.14740/jnr709

Liu, Q., Wang, X., and Yi, S. (2018). Pathophysiological changes of physical barriers of peripheral nerves after injury. *Front. Neurosci.* 12, 597. doi:10.3389/fnins.2018.00597

Ludolph, A. C., Bendotti, C., Blaugrund, E., Chio, A., Greensmith, L., Loeffler, J. P., et al. (2010). Guidelines for preclinical animal research in ALS/MND: A consensus meeting. *Amyotroph. Lateral Scler.* 11, 38–45. doi:10.3109/17482960903545334

Mammarella, N., Gatti, M., Ceccato, I., Di Crosta, A., Di Domenico, A., and Palumbo, R. (2022). The protective role of neurogenetic components in reducing stress-related effects during spaceflights: Evidence from the age-related positive memory approach. *Life (Basel)* 12, 1176. doi:10.3390/life12081176

Matsumura, T., Noda, T., Muratani, M., Okada, R., Yamane, M., Isotani, A., et al. (2019). Male mice, caged in the International Space Station for 35 days, sire healthy offspring. *Sci. Rep.* 9, 13733. doi:10.1038/s41598-019-50128-w

McCoy, E. S., Taylor-Blake, B., Street, S. E., Pribisko, A. L., Zheng, J., and Zylka, M. J. (2013). Peptidergic CGRPα primary sensory neurons encode heat and itch and tonically suppress sensitivity to cold. *Neuron* 78, 138–151. doi:10.1016/j.neuron.2013.01.030

Meltzer, S., Santiago, C., Sharma, N., and Ginty, D. D. (2021). The cellular and molecular basis of somatosensory neuron development. *Neuron* 109, 3736–3757. doi:10.1016/j.neuron.2021.09.004

Mhatre, S. D., Iyer, J., Puukila, S., Paul, A. M., Tahimic, C. G. T., Rubinstein, L., et al. (2022). Neuro-consequences of the spaceflight environment. *Neurosci. Biobehav. Rev.* 132, 908–935. doi:10.1016/j.neubiorev.2021.09.055

Murano, T., Hagihara, H., Tajinda, K., Matsumoto, M., and Miyakawa, T. (2019). Transcriptomic immaturity inducible by neural hyperexcitation is shared by multiple neuropsychiatric disorders. *Commun. Biol.* 2, 32. doi:10.1038/s42003-018-0277-2

Murano, T., Koshimizu, H., Hagihara, H., and Miyakawa, T. (2017). Transcriptomic immaturity of the hippocampus and prefrontal cortex in patients with alcoholism. *Sci. Rep.* 7, 44531. doi:10.1038/srep44531

Nagatomo, F., Terada, M., Ishioka, N., and Ishihara, A. (2014). Effects of exposure to microgravity on neuromuscular systems: A review. *Int. J. Microgravity Sci. Appl.* 31, 66–71. doi:10.15011/jasma.31.2.66

Nguyen, Y. T. K., Ha, H. T. T., Nguyen, T. H., and Nguyen, L. N. (2021). The role of SLC transporters for brain health and disease. *Cell. Mol. Life Sci.* 79, 20. doi:10.1007/s00018-021-04074-4

Okada, R., Fujita, S. I., Suzuki, R., Hayashi, T., Tsubouchi, H., Kato, C., et al. (2021). Transcriptome analysis of gravitational effects on mouse skeletal muscles under microgravity and artificial 1 g onboard environment. *Sci. Rep.* 11, 9168. doi:10.1038/s41598-021-88392-4

Paixão, S., Loschek, L., Gaitanos, L., Alcalà Morales, P., Goulding, M., and Klein, R. (2019). Identification of spinal neurons contributing to the dorsal column projection mediating fine touch and corrective motor movements. *Neuron* 104, 749–764.e6. doi:10.1016/j.neuron.2019.08.029

Pampalakis, G., Mitropoulos, K., Xiromerisiou, G., Dardiotis, E., Deretzi, G., Anagnostouli, M., et al. (2019). New molecular diagnostic trends and biomarkers for amyotrophic lateral sclerosis. *Hum. Mutat.* 40, 361–373. doi:10.1002/humu.23697

Paul, A. M., Overbey, E. G., da Silveira, W. A., Szewczyk, N., Nishiyama, N. C., Pecaut, M. J., et al. (2021). Immunological and hematological outcomes following protracted low dose/low dose rate ionizing radiation and simulated microgravity. *Sci. Rep.* 11, 11452. doi:10.1038/s41598-021-90439-5

Radstake, W. E., Baselet, B., Baatout, S., and Verslegers, M. (2022). Spaceflight stressors and skin health. *Biomedicines* 10, 364. doi:10.3390/biomedicines10020364

Renthal, W., Tochitsky, I., Yang, L., Cheng, Y. C., Li, E., Kawaguchi, R., et al. (2020). Transcriptional reprogramming of distinct peripheral sensory neuron subtypes after axonal injury. *Neuron* 108, 128–144.e9. doi:10.1016/j.neuron.2020.07.026

Rizzo, F., Riboldi, G., Salani, S., Nizzardo, M., Simone, C., Corti, S., et al. (2014). Cellular therapy to target neuroinflammation in amyotrophic lateral sclerosis. *Cell. Mol. Life Sci.* 71, 999–1015. doi:10.1007/s00018-013-1480-4

Rubio, M. A., Herrando-Grabulosa, M., Gaja-Capdevila, N., Vilches, J. J., and Navarro, X. (2022). Characterization of somatosensory neuron involvement in the $SOD1^{G93A}$ mouse model. *Sci. Rep.* 12, 7600. doi:10.1038/s41598-022-11767-8

Ruiz-Soto, M., Riancho, J., Tapia, O., Lafarga, M., and Berciano, M. T. (2020). Satellite glial cells of the dorsal root ganglion: A new 'guest/physiopathological target' in ALS. *Front. Aging Neurosci.* 12, 595751. doi:10.3389/fnagi.2020.595751

Sábado, J., Casanovas, A., Tarabal, O., Hereu, M., Piedrafita, L., Calderó, J., et al. (2014). Accumulation of misfolded SOD1 in dorsal root ganglion degenerating proprioceptive sensory neurons of transgenic mice with amyotrophic lateral sclerosis. *Biomed. Res. Int.* 2014, 1–13. doi:10.1155/2014/852163

Schütz, B. (2005). Imbalanced excitatory to inhibitory synaptic input precedes motor neuron degeneration in an animal model of amyotrophic lateral sclerosis. *Neurobiol. Dis.* 20, 131–140. doi:10.1016/j.nbd.2005.02.006

Sharma, N., Flaherty, K., Lezgiyeva, K., Wagner, D. E., Klein, A. M., and Ginty, D. D. (2020). The emergence of transcriptional identity in somatosensory neurons. *Nature* 577, 392–398. doi:10.1038/s41586-019-1900-1

Shiba, D., Mizuno, H., Yumoto, A., Shimomura, M., Kobayashi, H., Morita, H., et al. (2017). Development of new experimental platform 'MARS'-multiple artificial-gravity research system-to elucidate the impacts of micro/partial gravity on mice. *Sci. Rep.* 7, 10837. doi:10.1038/s41598-017-10998-4

Shorrock, H. K., Gillingwater, T. H., and Groen, E. J. N. (2019). Molecular mechanisms underlying sensory-motor circuit dysfunction in SMA. *Front. Mol. Neurosci.* 12, 59. doi:10.3389/fnmol.2019.00059

Sprowl, J. A., Ciarimboli, G., Lancaster, C. S., Giovinazzo, H., Gibson, A. A., Du, G., et al. (2013). Oxaliplatin-induced neurotoxicity is dependent on the organic cation transporter OCT2. *Proc. Natl. Acad. Sci. USA.* 110, 11199–11204. doi:10.1073/pnas.1305321110

Tamura, K., Sugita, S., Tokunaga, T., Minegishi, Y., and Ota, N. (2019). TRPM8-mediated cutaneous stimulation modulates motor neuron activity during treadmill stepping in mice. *J. Physiol. Sci.* 69, 931–938. doi:10.1007/s12576-019-00707-3

Tao, Q. Q., Wei, Q., and Wu, Z. Y. (2018). Sensory nerve disturbance in amyotrophic lateral sclerosis. *Life Sci.* 203, 242–245. doi:10.1016/j.lfs.2018.04.052

Usoskin, D., Furlan, A., Islam, S., Abdo, H., Lönnerberg, P., Lou, D., et al. (2015). Unbiased classification of sensory neuron types by large-scale single-cell RNA sequencing. *Nat. Neurosci.* 18, 145–153. doi:10.1038/nn.3881

Vaughan, S. K., Kemp, Z., Hatzipetros, T., Vieira, F., and Valdez, G. (2015). Degeneration of proprioceptive sensory nerve endings in mice harboring amyotrophic lateral sclerosis-causing mutations. *J. Comp. Neurol.* 523, 2477–2494. doi:10.1002/cne.23848

Vaughan, S. K., Sutherland, N. M., Zhang, S., Hatzipetros, T., Vieira, F., and Valdez, G. (2018). The ALS-inducing factors, TDP43A315T and SOD1G93A, directly affect and sensitize sensory neurons to stress. *Sci. Rep.* 8, 16582. doi:10.1038/s41598-018-34510-8

Vinsant, S., Mansfield, C., Jimenez-Moreno, R., Del Gaizo Moore, V., Yoshikawa, M., Hampton, T. G., et al. (2013a). Characterization of early pathogenesis in the SOD1(g93a) mouse model of ALS: Part I, background and methods. *Brain Behav.* 3, 335–350. doi:10.1002/brb3.143

Vinsant, S., Mansfield, C., Jimenez-Moreno, R., Del Gaizo Moore, V., Yoshikawa, M., Hampton, T. G., et al. (2013b). Characterization of early pathogenesis in the SOD1(g93a) mouse model of ALS: Part II, results and discussion. *Brain Behav.* 3, 431–457. doi:10.1002/brb3.142

Wu, H., Petitpré, C., Fontanet, P., Sharma, A., Bellardita, C., Quadros, R. M., et al. (2021). Distinct subtypes of proprioceptive dorsal root ganglion neurons regulate adaptive proprioception in mice. *Nat. Commun.* 12, 1026. doi:10.1038/s41467-021-21173-9

Yi, Y., Li, L., Song, F., Li, P., Chen, M., Ni, S., et al. (2021). L-tetrahydropalmatine reduces oxaliplatin accumulation in the dorsal root ganglion and mitochondria through selectively inhibiting the transporter-mediated uptake thereby attenuates peripheral neurotoxicity. *Toxicology* 459, 152853. doi:10.1016/j.tox.2021.152853

Yoshikawa, M., Aizawa, S., Oppenheim, R. W., and Milligan, C. (2022a). Neurovascular unit pathology is observed very early in disease progression in the mutant SOD1G93A mouse model of amyotrophic lateral sclerosis. *Exp. Neurol.* 353, 114084. doi:10.1016/j.expneurol.2022.114084

Yoshikawa, M., Ishikawa, C., Li, H., Kudo, T., Shiba, D., Shirakawa, M., et al. (2022b). Comparing effects of microgravity and amyotrophic lateral sclerosis in the mouse ventral lumbar spinal cord. *Mol. Cell. Neurosci.* 121, 103745. doi:10.1016/j.mcn.2022.103745

Yu, X., Ji, C., and Shao, A. (2020). Neurovascular unit dysfunction and neurodegenerative disorders. *Front. Neurosci.* 14, 334. doi:10.3389/fnins.2020.00334

Zholudeva, L. V., Abraira, V. E., Satkunendrarajah, K., McDevitt, T. C., Goulding, M. D., Magnuson, D. S. K., et al. (2021). Spinal interneurons as gatekeepers to neuroplasticity after injury or disease. *J. Neurosci.* 41, 845–854. doi:10.1523/JNEUROSCI.1654-20.2020